

We are IntechOpen, the world's leading publisher of Open Access books Built by scientists, for scientists

4,800

Open access books available

122,000

International authors and editors

135M

Downloads

Our authors are among the

154

Countries delivered to

TOP 1%

most cited scientists

12.2%

Contributors from top 500 universities



WEB OF SCIENCE™

Selection of our books indexed in the Book Citation Index
in Web of Science™ Core Collection (BKCI)

Interested in publishing with us?
Contact book.department@intechopen.com

Numbers displayed above are based on latest data collected.
For more information visit www.intechopen.com



Highly Efficient Biomass Utilization with Solid Oxide Fuel Cell Technology

Yusuke Shiratori^{1,2}, Tran Tuyen Quang¹, Yutaro Takahashi¹,
Shunsuke Taniguchi^{1,3} and Kazunari Sasaki^{1,2,3}

¹Department of Mechanical Engineering, Faculty of Engineering, Kyushu University

²International Institute for Carbon-Neutral Energy Research (WPI), Kyushu University

³International Research Center for Hydrogen Energy, Kyushu University
Japan

1. Introduction

Mankind has been consuming plants, i.e. biomass, as an energy source for living and developing on earth from the paleolithic period to early the modern period. Consumption of bio-energy does not change the atmospheric environment because carbon dioxide emitted by the use of bio-energies will be used by plants through the photosynthesis (Züttel, 2008). Since 1769 James Watt significantly improved the steam engine, invented by Thomas Savery in 1698. The steam engine was widely introduced for producing mechanical work from chemical energy of fuels, i.e. mineral coal and wood. More practical heat engines, external and internal combustion engines, have served for developing of human society for almost two and a half centuries. Since the Otto-Langen engine was first introduced in 1867, human society has developed using the internal combustion engines (IC engines), which nowadays are used worldwide for transportation, manufacture, power generation, construction and farming. However, large consumption of fossil fuels may bring about environmental pollution and climate change.

Fuel cells are electrochemical devices that convert chemical energy of fuels directly into electrical energy without the Carnot limitation that limit IC engines. Even in the smallest power range of less than 10 kW, fuel cells exhibit electrical efficiencies of 35-50 %LHV (lower heating value), while being silent, whereas engines and microturbines show low electrical efficiency of 25-30%LHV and high levels of noise. Therefore, the fuel cell which can be operated with very low environmental emission levels, is regarded as a promising candidate for a distributed power source in the next generation. Although most fuel cells operate with hydrogen as a fuel, solid oxide fuel cells (SOFCs) operated in a high temperature range between 600 and 900 °C accept the direct use of hydrocarbon fuels. Hydrocarbon fuels directly supplied to SOFCs are reformed in the porous anode materials producing H₂-rich syngas, which is subsequently used to generate electricity and heat through electrochemical oxidation (Steele & Heinzl, 2001; Sasaki & Teraoka, 2003). This type of SOFC, so called internal reforming SOFC (IRSOFC), enables us to simplify the SOFC system. Electrochemical performances of IRSOFC have been reported for gaseous and liquid fossil fuels such as methane (Park et al., 1999), propane (Iida et al., 2007), n-dodecane

(Kishimoto et al., 2007), synthetic diesel (Kim et al., 2001), crude oil and jet fuel (Zhou et al., 2004). Highly efficient fuel cells operated by fossil fuels can certainly contribute to the suppression of environmentally harmful emissions, but in view of exhaustion of fossil resources, the utilization of renewable bio-energies should be more promoted. Direct feeding of biofuels to SOFC gives an environmental-friendly, compact and cost-effective energy conversion system. Biogas derived primarily from garbage is one of the most attractive bio-energies for SOFC (Van herle et al., 2004a; Shiratori et al., 2008, 2010a, 2010b). Recently, Shiratori et al. (2010) has demonstrated the stable operation of an IRSOFC operating on non-synthetic biogas over one month using an anode-supported button cell. On the other hand, the use of liquid biofuels is also attractive due to their easy storage and transportation with high energy density. Tran et al. (2011) has demonstrated the stable operation of an IRSOFC operating on practical palm-biodiesel over 800 h, also using an anode-supported button cell.

In this chapter, performances of IRSOFCs operating on biofuels are summarized and roadblocks to overcome for the realization of this type of highly-efficient carbon-neutral fuel cell are mentioned.

2. Sustainable society using internal reforming SOFC (IRSOFC) running on biofuels (*Bio*-SOFC)

Although the conventional large scale power system provides us with a stable electric power supply, the associated large consumption of fossil fuels and release of large amount of waste heat are unfit for social and environmental needs in recent years. Now, the role of biomass, having the largest exploitation potential among renewable energy resources, becomes very important. Of course, the use of edible plants is highly restricted, but the use of organic wastes is highly desirable. Biogas and biodiesel fuels (BDFs) are attractive alternative fuels which can be produced from bio-wastes, and their spread will generate synergistic effects to create new industries and employment in their production and refinement processes.

Among fuel cells, the SOFC is the only technology capable of converting bio-energies directly to electricity without an external fuel reformer (Staniforth et al. 1998). As for the low temperature fuel cells like polymer electrolyte fuel cell (PEFC), the external reforming process is essential prior to electrochemical conversion of biofuels to electricity. Superiority of an IRSOFC running on biofuels (hereafter called *Bio*-SOFC) is described in Fig. 1. By selecting red arrows in this figure social needs are satisfied. Our final goal is to establish a microgrid system as shown in Fig 2 using *Bio*-SOFC as major distributed generators providing heat and power on site. These distributed *Bio*-SOFCs can contribute to leveling of the unstable power supply from solar and wind energies. However, breakthroughs are necessary to realize the *Bio*-SOFC system.

3. Solid oxide fuel cell (SOFC)

The solid oxide fuel cell (SOFC) offers a highly efficient and fuel-flexible technology for distributed power generation and combined heat and power (CHP) systems, and it is obviously promising technology for utilizing biofuels. In this section, SOFC technologies are briefly reviewed from fundamentals to current status of development.

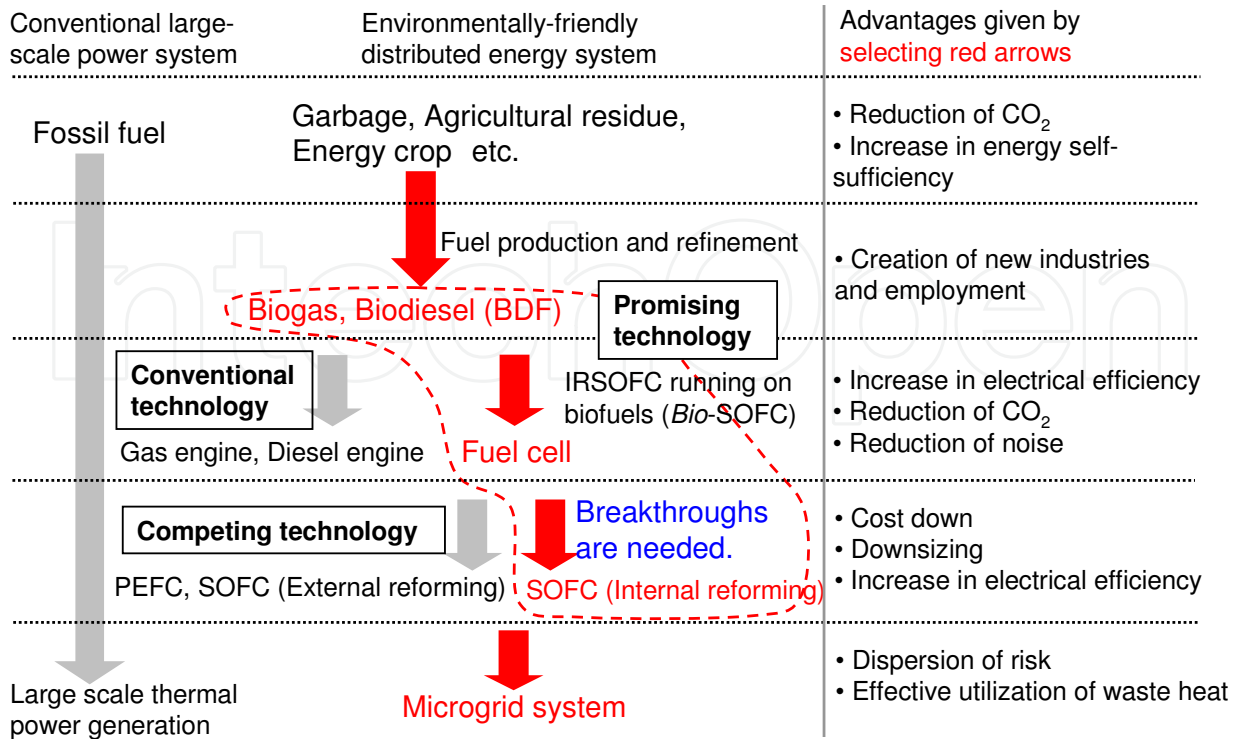


Fig. 1. Superiority of IRSOFC running on biofuels (*Bio*-SOFC), a promising candidate as a distributed generator in the next generation.

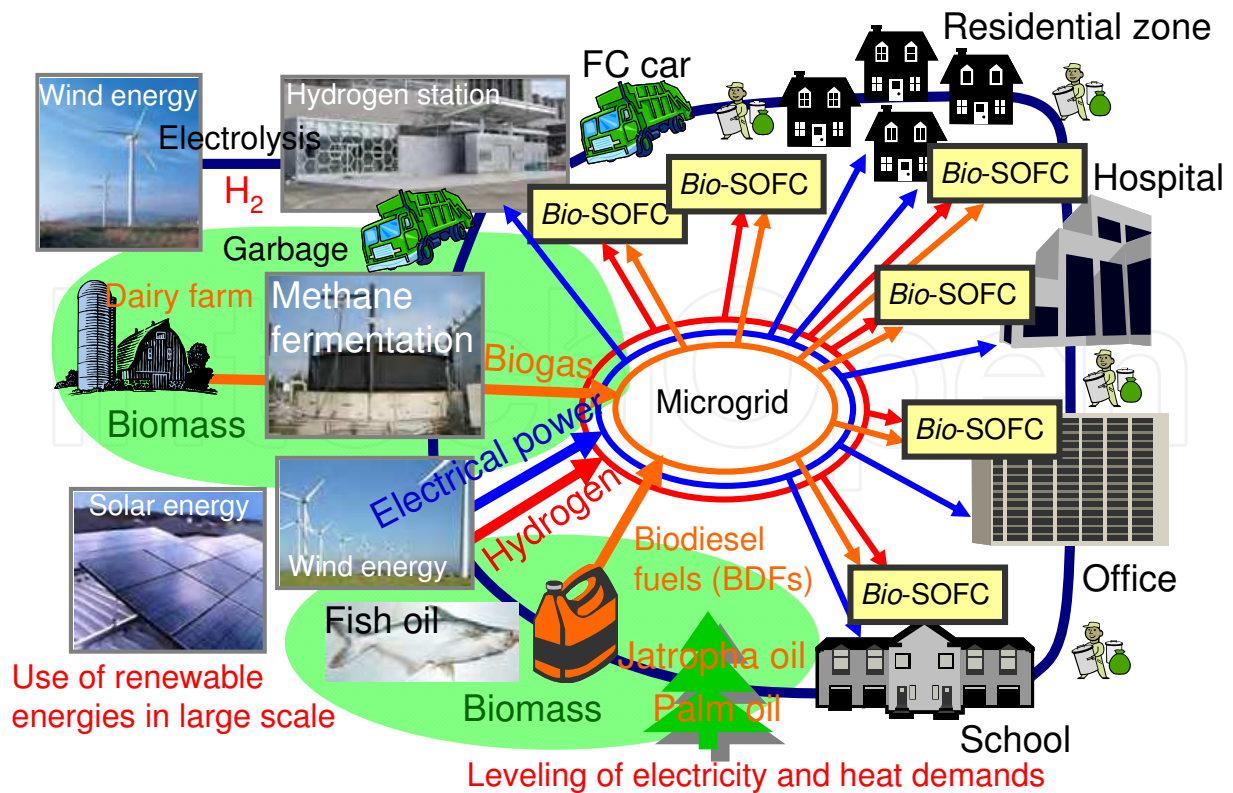


Fig. 2. Microgrid system using *Bio*-SOFC as a major distributed power source.

3.1 Operation mechanism

A fuel cell in general converts chemical energy of the fuel directly into electrical energy without converting it to mechanical energy. Therefore, the fuel cell has potential of attaining higher electrical conversion efficiency than those of conventional technologies such as heat engines limited by Carnot efficiency. Fig. 3 shows the principle of SOFC operation. The basic unit of an SOFC, i.e. cell, consists of an electrolyte sandwiched with two electrodes, anode and cathode. In the electricity generation process, an oxide ion O^{2-} is generated from oxygen in air via the cathodic reaction (1).



Normally, SOFCs are operated in the temperature range between 600 and 900 °C in which electrolytes composed of doped metal oxides can exhibit rather high oxygen ion conductivity. Oxygen ions generated in the cathode are transported to the anode side through the dense electrolyte and are used to electrochemically oxidize a fuel, here hydrogen, in the anodic reaction (2).



In the high temperature SOFC, not only hydrogen but also carbon monoxide can contribute to the generation of electricity (3). Hydrogen and carbon monoxide can be produced by steam reforming or partial oxidation of hydrocarbon fuels on the Ni-based anode material, therefore in principle hydrocarbon fuels can be directly supplied to SOFC without using a pre-reformer.

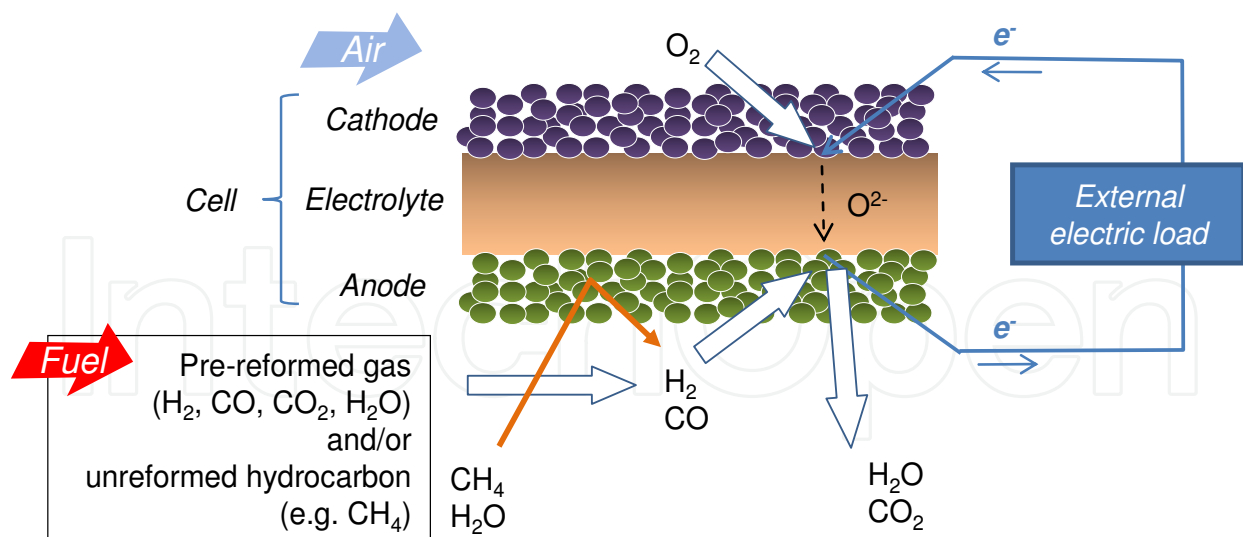


Fig. 3. Principle of SOFC operation.

The electromotive force of fuel cell, E , derived from the difference in the partial pressure of oxygen, $p(O_2)$, between cathode and anode sides can be expressed by the Nernst equation (4).

$$E = (RT/4F) \ln \{ p(O_2, c)/p(O_2, a) \}, \quad (4)$$

where R is the gas constant and T is absolute temperature. a and c denote anode and cathode sides, respectively. Theoretically, E is approximately 1 volt, and the ideal electrical efficiency can be calculated by $\Delta G/\Delta H$, where ΔG and ΔH are Gibbs free energy change and enthalpy change of the hydrogen combustion reaction (5), respectively. At the operating temperature of 800 °C ideal efficiency becomes 70%LHV.



The actual electrical efficiency of an SOFC (40-50 %LHV) is always lower than the ideal value because fuel utilization (U_f) can not be increased up to 100 % in the practical SOFC system and the contribution of the internal resistances such as resistances of the materials themselves, contact resistances and electrode reaction resistances is not negligible. However, in the small size fuel cell systems, the heat generation, including the intrinsic heat release, $\Delta H - \Delta G$, can be utilized effectively on site leading to overall efficiency above 80 %LHV.

The SOFC has the following advantages because of its high operating temperature. Various kinds of fuel, such as natural gas, liquefied petroleum gas, kerosene and biofuels, etc. can be utilized with a simple fuel processing system. Even direct feeding of such practical fuels is theoretically possible. Higher electrical efficiency above 50 %LHV can be obtained by setting higher fuel utilization. Overall efficiency can be enhanced by using the heat released from the cell for the fuel reforming process, in which endothermic steam reforming proceeds as a main reaction. This kind of energy recycle is possible because the operational temperature of SOFC is nearly the same as that of the reformer. In addition, further enhancement of electrical efficiency is expected by using residual fuel and water vapor in a downstream gas turbine and steam turbine. High quality heat from the high temperature SOFC system can also be utilized effectively for hot water supply as well as reformer.

3.2 Component materials of SOFC and stack configurations

In Table 1, requirements for component materials of a cell and interconnector are summarized. Typical materials are also listed in this table. The electrolyte has to be gas-tight to prevent leakage of fuel and oxidant gases. Both electrodes have to be porous to provide electrochemical reaction sites. The interconnector plays a role of electrically connecting the anode of one cell and the cathode of the adjoining cell, and also separating the fuel in the anode side from the oxidant in the cathode side. Component materials must be heat resistant and durable in the highly oxidative and reductive atmospheres for cathode and anode sides, respectively.

To fabricate a cell, powders of these component materials are formed into desired shapes by general ceramic processing such as extrusion, slip casting, pressing, tape casting, printing and dip coating (Stöver et al., 2003). Subsequently, the resulting "green" ceramics undergo heat-treatments. High temperature sintering processing above 1300 °C is normally required to obtain a dense and gas tight electrolyte layer.

In an SOFC, all solid state fuel cell, various types of cell configuration have been designed and classified by support materials and shapes as summarized in Table 2. The SOFC has a laminate structure of thin ceramic layers, therefore a support material is necessary to ensure the mechanical stability. Anode-supported, electrolyte-supported, cathode-supported, metal-supported and nonconductive ceramic-supported (segmented-in-series) types have been developed. From the viewpoint of cell shape, there are roughly three types, i.e., planar, flat tubular and tubular types.

Component materials		Requirements	Typical materials
Cell	Electrolyte	Dense (Gas tight), Ionically conductive	Y ₂ O ₃ -stabilized ZrO ₂ (YSZ), Sc ₂ O ₃ -stabilized ZrO ₂ (ScSZ), Gd ₂ O ₃ doped CeO ₂ (GDC), (La,Sr)(Ga,Mg)O ₃ (LSGM))
	Anode	Porous, Electrochemically active, Electronically conductive	Ni-YSZ, Ni-ScSZ, Ni-GDC
	Cathode	Porous, Electrochemically active, Electronically conductive	(La,Sr)MnO ₃ , (La,Sr)(Fe,Co)O ₃
Interconnector		Dense (Gas tight), Electronically conductive	(La,Sr)CrO ₃ , (La,Ca)CrO ₃ , (Sr,La)TiO ₃ , Stainless steel

Table 1. Requirements for component materials and typical materials used to fabricate SOFC.

Support materials	Cell shape		
	Planar	Flat tubular	Tubular
Anode-supported	Versa Power Systems, Ceramic Fuel Cells, Topsoe Fuel Cell, Nippon Telegraph and Telephone, NGK Spark Plug	Kyocera	Acumentrics, TOTO
Electrolyte-supported	Hexis, Mitsubishi Materials		
Cathode-supported		Siemens Power Generation	Siemens Power Generation, TOTO
Metal-supported	Ceres Power		
Nonconductive ceramic-supported (Segmented-in-series *)		Rolls-Royce Fuel Cell Systems, Tokyo gas	Mitsubishi Heavy Industries

* Cells are formed in series on a nonconductive porous ceramics.

Table 2. Various SOFC configurations.

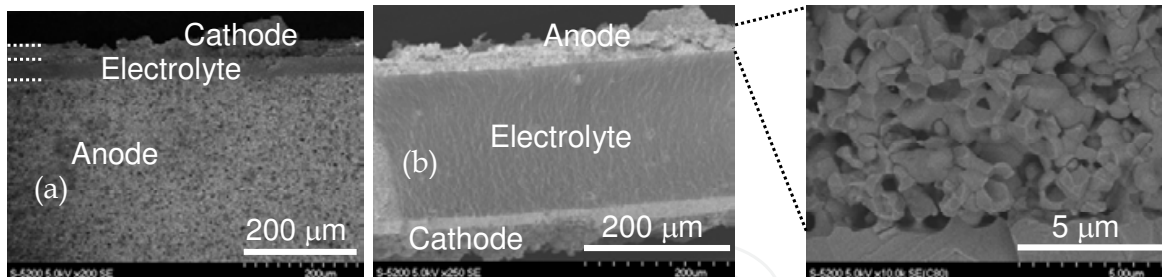


Fig. 4. FESEM images of (a) anode-supported cell and (b) electrolyte-supported cell.

Resistance of the electrolyte dominates the internal voltage loss in many cases, thus making thinner electrolytes is a key technology to achieve better performance especially at lower operating temperatures. For example, an anode-supported cell (Fig. 4a), in which a thin electrolyte layer with a thickness of around $15\ \mu\text{m}$ is formed on the anode substrate with a thickness of $1\ \text{mm}$, enables operation of an SOFC around $200\ \text{K}$ lower in temperature as compared to an electrolyte-supported cell (Fig. 4b) (Steele & Heinzel, 2001).

There are also various types of stack structures with different flow directions of electric current, fuel and air, as shown in Fig. 5. The planar type (Fig. 5a) can achieve higher current density and lower manufacturing cost, but it has lower tolerance to thermal stress. Flat tubular type (Fig. 5b) exhibits higher durability than planar type because the area for gas seal is smaller compared to planar type without changing the direction of electric current. This type enables downsizing of a SOFC stack but is not suitable for hundred kW class large systems due to the mechanical properties of the interconnector material. The segmented-in-series type (Fig. 5c) has the advantage of scalability because gas seals and electrical connections between the adjacent cells are already completed. However, this structure is complicated and a lot of optimization is required for precise fabrication.

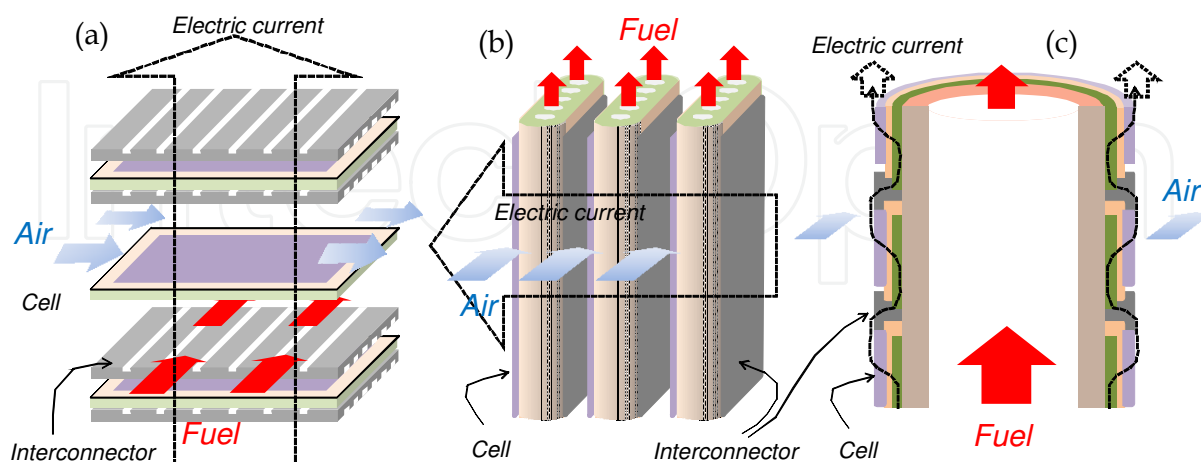


Fig. 5. Structures of SOFC stack; (a) anode-supported planar type (b) anode-supported flat tubular type and (c) segmented-in-series tubular type.

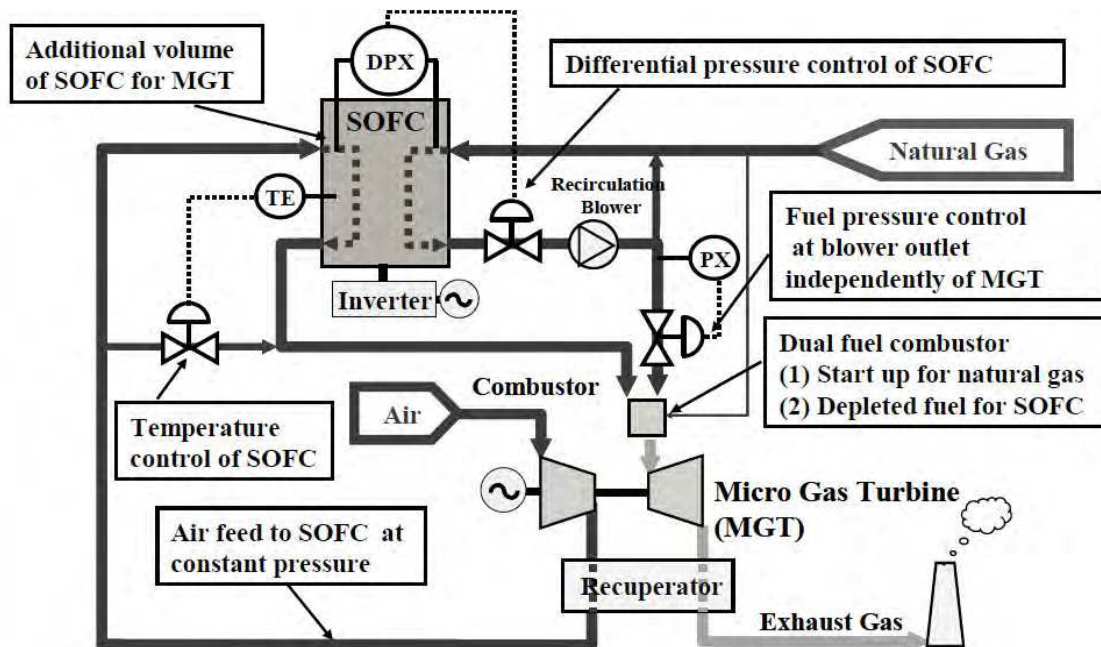


Fig. 6. Flow diagram of 200 kW-class SOFC-micro gas turbine combined system developed by Mitsubishi Heavy Industries (Yoshida et al., 2011).

Large scale SOFC systems are being developed aiming for a distributed electrical power plant with high energy conversion efficiency. Mitsubishi Heavy Industries (JP) has developed a 200 kW class micro gas turbine hybrid system as shown in Fig. 6 with a maximum efficiency of 52.1% LHV, and a maximum gross power of 229 kW-AC was achieved with natural gas as a fuel. Their final goal is to achieve electrical efficiency of 70% by developing large-scale power generation system in which the SOFC integrates with gas turbines and steam turbines (Yoshida et al., 2011). Rolls-Royce Fuel Cell Systems (GB) is designing a stationary 1 MW SOFC power generation system based on their segmented-in-series cell stack named Integrated-Planar SOFC technology (Haberman et al., 2011; Gardner et al., 2000). FuelCell Energy (US) is developing SOFC power plants, currently utilizing SOFC stacks developed by Versa Power Systems (CA). Their ultimate goal is to develop Multi-MW SOFC power plants suitable for integration with coal gasifiers and capable of capturing > 90% of carbon in coal syngas (Huang et al., 2011).



Fig. 7. Appearances of installation sites of residential SOFC CHP systems under demonstrative research project in Japan (Hosoi et al., 2011).

Small scale SOFCs of 1 -2 kW class are now being developed all over the world, aiming at early commercialization of residential CHP systems (Fig. 7). City gas is generally used as a fuel with high overall efficiency more than 80 %LHV obtained by utilizing both electricity and heat on site. In Japan, a demonstrative research project is now being carried out in which Kyocera (JP), Tokyo gas (JP) and TOTO (JP) participate as manufacturers of SOFC stacks. More than 200 systems have been installed on actual residential sites as of FY2010. In this project, reductions of primary energy consumption and CO₂ emission by 16 and 34 %, respectively, were demonstrated (Hosoi et al., 2011). Until now, long-term operation over 25,000 h has been demonstrated, and potential of 40,000 h durability has been confirmed. Ceramic Fuel Cells (AU) is manufacturing the residential system called BlueGen which can deliver initial electrical efficiency of 60 %LHV at 1.5 kW-AC, and exhibited 55 % efficiency after 1 year operation (Föger et al., 2010; Payne et al., 2011). Hexis Ltd. (CH) had operated 1 kW class system for 28,000 h (Mai et al., 2011). Acumentrics (US) (Byham et al., 2010) and Ceres Power (GB) are also developing residential SOFC systems (Leah et al., 2011).

For the spread of these SOFC systems, further enhancements of electrical efficiency, fuel flexibility and thermomechanical reliability are essential. In this chapter, these challenges are summarized taking our effort, application of biofuels to SOFC, as a good example of advancements.

4. Performance of IRSOFC operating on biofuels (*Bio*-SOFCs)

4.1 Experimental

4.1.1 SOFC single cell used in the tests

Ni-yttria stabilized zirconia cermet (Ni-YSZ) is the most popular material for SOFC anodes. However, it has been reported that Ni-scandia stabilized zirconia (Ni-ScSZ) offers better catalytic performance and can suppress coking when hydrocarbon fuels are supplied to SOFC (Ke et al., 2006). Thus, we used anode-supported type cells based on the anode/electrolyte bilayer (half cell) of Ni-ScSZ/ScSZ to evaluate the electrochemical and catalytic performance of IRSOFCs operating on biofuels (*Bio*-SOFCs). Two types of half cells, button cell with diameter of 20 mm and square-shaped cells with area of 5 x 5 cm² purchased from Japan fine ceramics were used to fabricate single cells. The cells consist of ScSZ electrolyte with a thickness of 14 μm sintered on a porous anode support (mixture of NiO and ScSZ (NiO:ScSZ = 5.6:4.4)) with a thickness of 800 μm. A mixture of (La_{0.8}Sr_{0.2})_{0.98}MnO₃ (> 99.9 %, Praxair, USA, abbreviated by LSM) and ScSZ (Daiichi Kigenso Kagaku Kogyo, Japan) with a weight ratio of 1:1 was adopted as a cathode functional layer and coarse LSM was applied as a cathode current collector layer. Porous cathodes with the area of 0.8 x 0.8 and 4 x 4 cm² for button and square-shaped cells, respectively, were obtained by sintering process at 1200 °C for 3 h. Component materials of the single cells were summarized in Table 3.

Component materials	Composition	Thickness / μm
Electrolyte	10 mol% Sc ₂ O ₃ -1 mol% CeO ₂ -ZrO ₂ (ScSZ)	14
Anode functional layer	56%NiO-44%ScSZ	26
Anode substrate	56%NiO-44%ScSZ	800
Cathode	50%(La _{0.8} Sr _{0.2}) _{0.98} MnO ₃ (LSM)-50%ScSZ	~30
Cathode current collector layer	LSM	~30

Table 3. Component materials of the anode-supported single cells (Shiratori et al., 2010b).

4.1.2 IRSOFC operating on biogas

The SOFC testing system and automatic gas chromatograph were connected to the methane fermentation reactor placed in Tosu Kankyo Kaihatsu Ltd. as shown in Fig. 8 (Shiratori et al., 2010a). Garbage collected in Tosu-city of Saga prefecture was mixed with water resulting in waste slurry. After materials unsuitable for anaerobic fermentation were filtered out, cattle manure was added to the slurry followed by the treatment with acid and methane fermentation processes to produce biogas (mixture of CH₄ and CO₂) containing 790 ppm H₂S. The raw biogas was passed through a desulfurizer packed with FeO pellets 20 cm³ in size. The typical composition of desulfurized biogas sampled from the fermentation reactor is listed in Table 4. The concentration of H₂S was less than 0.5 ppm. The concentrations of the other fuel impurities, CH₃SH, Cl₂, HCl, NH₃ and siloxane, were below the detection limits (2 ppb, 60 ppb, 0.4 ppm, 0.6 ppm and 10 ppb, respectively), indicating that this gas can be fed directly into a SOFC (Haga et al., 2008). In any case, 1 ppm level H₂S contamination must be taken into account even after desulfurization treatment. The experimental setup for testing IRSOFC operating on biogas has been described elsewhere (Shiratori et al., 2010a). The pressure controlled real biogas (0.1 MPa) was directly distributed to the SOFC at 800 °C and the gas chromatograph with flow rates of 25 and 140 ml min⁻¹, respectively, in order to evaluate the electrochemical performance with simultaneous monitoring of biogas composition. In this experiment, water vapor in the real biogas was removed by a cold trap thermostated at 0 °C. Dry air was supplied to the cathode side with a flow rate of 50 ml min⁻¹

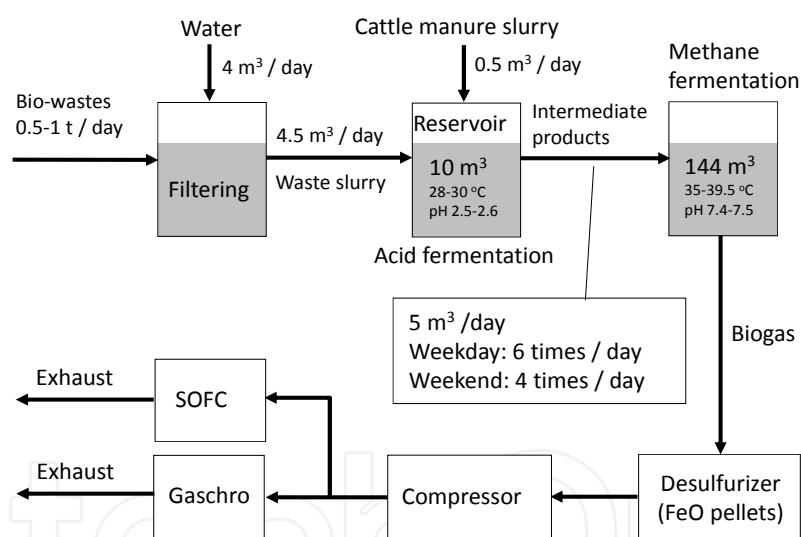


Fig. 8. Connection of SOFC test system and gas chromatograph with the methane fermentation reactor in Tosu-city, Japan (Shiratori et al., 2010a, 2010b).

Gaseous species	Concentration
CH ₄	62.6 vol %
CO ₂	35.7 vol %
H ₂ O	1.62 vol %
N ₂	0.09 vol %
H ₂	99 vol ppm
H ₂ S	< 0.5 ppm

Table 4. Typical composition of the actual desulfurized biogas (Shiratori et al., 2010a).

4.1.3 IRSOFC operating on biodiesel fuels (BDFs)

Palm-, jatropha- and soybean-biodiesel fuels (BDFs) were produced from refined palm-, jatropha- and soybean-oils, respectively, at Bandung Institute of Technology, Indonesia (ITB). The main chemical components of the BDFs are listed in Table 5.

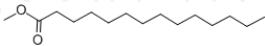
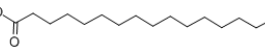
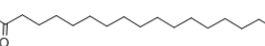
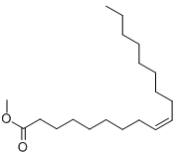
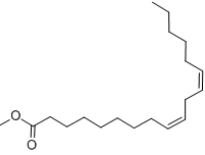
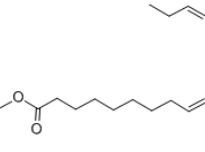
Formula	Structure	Concentration / wt %		
		Palm-BDF	Jatropha-BDF	Soybean-BDF
Myristic acid methyl ester $C_{15}H_{30}O_2$ (C14:0)		2.73	0.07	0.14
Palmitic acid methyl ester $C_{17}H_{34}O_2$ (C16:0)		39.1	14.6	11.0
Stearic acid methyl ester $C_{19}H_{38}O_2$ (C18:0)		4.21	6.55	3.21
Oleic acid methyl ester $C_{19}H_{36}O_2$ (C18:1)		40.4	39.9	24.4
Linoleic acid methyl ester $C_{19}H_{34}O_2$ (C18:2)		12.2	37.6	54.0
Linolenic acid methyl ester $C_{19}H_{32}O_2$ (C18:3)		0.26	0.19	5.75

Table 5. Main components in the biodiesel fuels applied to SOFC (Shiratori et al., 2011).

Table 6 shows the concentrations of saturated and unsaturated components in the BDFs and their average structures. Palm-BDF consisted mainly of 46.8 % saturated fatty acid methyl esters (FAMES) and 40.8 % mono-unsaturated FAMES. Jatropha- and soybean-BDFs contained a higher amount of unsaturated FAMES compared to palm-BDF. Jatropha-BDF consisted mainly of 40.9 % mono-unsaturated FAMES and 37.6 % di-unsaturated FAME. Soybean-BDF consisted mainly of 24.8 % mono-unsaturated FAMES and 54.0 % di-unsaturated FAME. Soybean-BDF not only contained higher amount of di-unsaturated FAME compared to jatropha-BDF but also contained a rather high amount of tri-unsaturated FAME (5.75 % linolenic fatty acid methyl ester). All BDFs had almost the same physical properties similar to petro-diesel. The experimental setup for testing the IRSOFC running on BDFs has been described elsewhere (Shiratori et al., 2011; Tran et al., 2011). Dry air was supplied to the cathode side with the flow rate of 150 ml min⁻¹. BDFs and H₂O were supplied to the anode side with the flow rates of 6 and 21-22 μl min⁻¹, respectively. BDFs

were evaporated and mixed with H₂O at 600 °C and then fed to the anode side together with nitrogen carrier gas with the flow rate of 50 ml min⁻¹.

	Concentration / wt %		
	BDFs		
	Palm-BDF	Jatropha-BDF	Soybean-BDF
Saturated	46.8	21.4	15.4
Unsaturated	53.2	78.6	84.6
Mono-	40.8	40.9	24.8
Di-	12.2	37.6	54.0
Tri-	0.26	0.19	5.75
Average structure	C _{18.0} H _{34.8} O ₂	C _{18.7} H _{35.0} O ₂	C _{18.8} H _{34.5} O ₂

Table 6. Composition of saturated and unsaturated components in the tested BDFs (Shiratori et al., 2011).

The C-H-O diagram (see Fig. 9) clearly shows that unless a generous amount of oxidant is added, biogas (CH₄/CO₂ = 1.5) and BDF will form coke on the anode material during SOFC operation. We added air and water to gaseous biogas and liquid BDF, respectively, to avoid carbon deposition from the thermodynamic point of view.

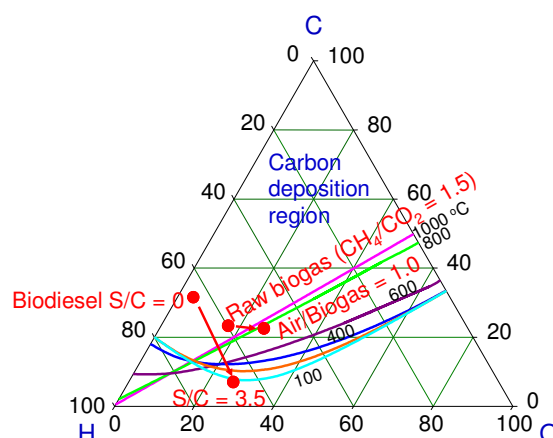


Fig. 9. C-H-O ternary diagram showing the possibility of coking when the biofuels are fed directly to SOFC (Sasaki & Teraoka, 2003).

4.2. Long term test of *Bio*-SOFCs

4.2.1 IRSOFC operating on biogas

The main reactions involved in an IRSOFC running on biogas are listed in Table 7. Internal dry reforming of CH₄ (reaction 1) proceeds on a Ni-based anode using CO₂ inherently included in biogas without an external reformer. Then, the produced H₂ and CO are electrochemically oxidized to produce electricity (reactions 2 and 3) (Shiratori et al., 2009a).

1	CH ₄ + CO ₂ → 2CO + 2H ₂	Dry reforming
2	H ₂ + O ²⁻ → H ₂ O + 2e ⁻	Electrochemical oxidation
3	CO + O ²⁻ → CO ₂ + 2e ⁻	Electrochemical oxidation

Table 7. Main reactions involved in IRSOFC running on biogas (Shiratori et al., 2009a).

Only a few reports have provided the performance of IRSOFCs operating on biogas (Staniforth et al., 2000; Shiratori et al., 2008; Girona et al., 2009; Lanzini & Leone, 2010a), because carbon formation thermodynamically can take place on the anode material. Staniforth et al. (2000) has reported the results of direct-feeding of landfill biogas (general CH₄-rich biogas). However, that was a short term experiment and not continuous feeding of as-produced real biogas. To avoid coking, pre-reforming of biogas is generally required (Van herle et al., 2004b). Recently, development of a new fermentation path producing H₂-rich biogas (Leone et al., 2010) and highly active catalysts to assist biofuel reforming (Xuan et al., 2009; Yentekakis et al., 2006; Zhou et al., 2007) have been reported. Heretofore, we have succeeded in stable operation of an IRSOFC running on actual biogas produced in waste treatment center using Ni-ScSZ cermet as an anode material without any support catalysts.

Figure 10a shows the cell voltages of IRSOFC operating on biogas measured at 200 mA cm⁻². Simulated biogas with the CH₄/CO₂ ratio of 1.5 led to a stable cell voltage above 0.8 V for 800 h. The degradation rate of only 0.4 %/1000 h proved that the biogas-fueled SOFC can be operated with an internal reforming mode. For the real biogas generated from the methane fermentation reactor, rather high voltage comparable to that obtained by simulated biogas was achieved for 1 month, although there is a voltage fluctuation. Monitoring of biogas composition simultaneously with the cell voltage (Fig. 10b) revealed that voltage fluctuation (a maximum of 50 mV level) appeared in synchronization with the fluctuation of CH₄/CO₂ ratio. An abrupt increase in CO₂ concentration induced temporarily decreased cell voltage. The CH₄/CO₂ ratio in the real biogas fluctuated between 1.4 and 1.7 which corresponds to CH₄ concentration range between 58 and 63 vol%. The biogas composition is influenced by many factors, for example, type of organic wastes, physical states and operational conditions of methane fermentation such as temperature and pH of the waste slurry.

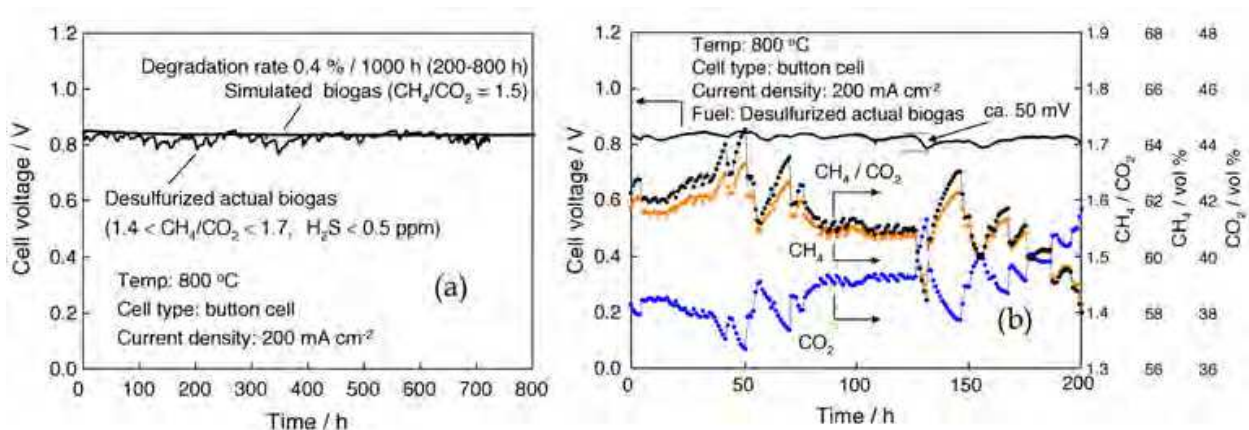


Fig. 10. Performance of IRSOFC operating on biogas (Shiratori et al., 2009a); (a) the results measured at 800 °C using anode-supported button cells and (b) voltage fluctuation in synchronization with the fluctuation of biogas composition during the long term test (initial 200 h of (a)).

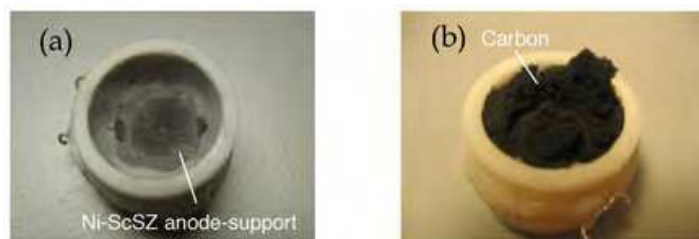


Fig. 11. Anode-supported cells after long term test shown in Fig. 10a using (a) simulated and (b) practical biogases.

From the thermodynamic point of view, a CH_4/CO_2 ratio of 1.5 should cause coking at 800°C , however carbon formation did not occur on the anode support for simulated biogas even after 800 h as shown in Fig. 11a. Provided that a fuel cell current is applied, this fuel composition (see Fig. 9) close to the border of the carbon deposition region may not cause coking. As for the real biogas, severe coking occurred during the long term test (Fig. 11b). The trigger of the coking was trace H_2S (< 0.5 ppm) in the real biogas which can cause deactivation of Ni catalyst for the dry reforming of methane (Sasaki et al., 2011; Shiratori et al., 2008). Acceleration of carbon deposition in the presence of trace H_2S was also reported for SOFCs operated with partially-reformed CH_4 -based fuels (Yuki et al., 2009). Although a threshold of maximum H_2S concentration tolerance for Ni-stabilized zirconia cermet anode must be provided in future work, total sulfur concentration should be reduced to less than 0.1 ppm level by employing an optimum desulfurization process.

4.2.2 IRSOFC operating on biodiesel fuel (BDF)

The main reactions inferred in the steam reforming of BDF are listed in Table 8 (Nahar, 2010). Steam reforming (reaction 1) produces H_2 and CO , and pyrolysis (reaction 2) produces light hydrocarbons (C_xH_y) and coke as well as H_2 and CO may occur as competing reactions. Both reactions are endothermic, more promoted at higher temperatures. Steam reforming is a heterogeneous reaction catalyzed by Ni, whereas pyrolysis, a non-catalytic gas phase reaction, tends to occur at water-lean regions or on the deactivated surface of the Ni-based anode. Excess H_2O reacts not only with the light hydrocarbons (reaction 3) but also with the produced CO (reaction 4) to form further H_2 . Reactions 5 and 6 are exothermic hydrogenation reactions which consume H_2 and produce CH_4 . Reactions 7 and 8 are endothermic gasification reactions of coke. While $\text{S}/\text{C} = 3.5$ is thermodynamically out of the carbon deposition region (see Fig. 9), contributions of reactions 5, 7 and 8 are not negligible once carbon is deposited on the anode surface.

1	$\text{C}_n\text{H}_m\text{O}_2 + (n-2)\text{H}_2\text{O} \Leftrightarrow (n+m/2-2)\text{H}_2 + n\text{CO}$	Steam reforming
2	$\text{C}_n\text{H}_m\text{O}_2 \Leftrightarrow \text{gases } (\text{H}_2, \text{CO}, \text{C}_x\text{H}_y) + \text{coke}$	Pyrolysis
3	$\text{C}_x\text{H}_y + x\text{H}_2\text{O} \Leftrightarrow x\text{CO} + (x+y/2)\text{H}_2$	Steam reforming
4	$\text{CO} + \text{H}_2\text{O} \Leftrightarrow \text{H}_2 + \text{CO}_2$	Water-gas shift
5	$\text{C} + 2\text{H}_2 \Leftrightarrow \text{CH}_4$	Hydrogenation
6	$\text{CO} + 3\text{H}_2 \Leftrightarrow \text{CH}_4 + \text{H}_2\text{O}$	Hydrogenation
7	$\text{C} + \text{H}_2\text{O} \Leftrightarrow \text{CO} + \text{H}_2$	Coke gasification
8	$\text{C} + \text{CO}_2 \Leftrightarrow 2\text{CO}$	Boudouard-reaction

Table 8. Main reactions involved in steam reforming of biodiesel fuel (Nahar, 2010).

Figure 12 shows the cell voltage of an IRSOFC operating on wet palm-BDF ($S/C = 3.5$) measured at 0.2 A cm^{-2} . Stable operation with a degradation rate of about 0.1 mV h^{-1} (approx. $1.5 \text{ \%}/100 \text{ h}$) was recorded. Total ohmic resistance of the cell, R_{IR} , total polarization resistance, R_P and the internal resistance of the cell, R_{int} (the sum of R_{IR} and R_P), measured under open circuit condition are also plotted in Fig. 12. R_{IR} and R_P increased linearly with operating time. The increasing rate of R_P , which is associated with activation and concentration overvoltages, is $0.15 \text{ m}\Omega \text{ cm}^2 \text{ h}^{-1}$, smaller than that of R_{IR} ($0.21 \text{ m}\Omega \text{ cm}^2 \text{ h}^{-1}$), indicating that the gradual loss of electrical contact was the main reason of the degradation. In this durability test, distinct morphology change and coking were not detected inside of the porous Ni-ScSZ anode support (see Fig. 14).

The composition of the anode off-gas (reformate gas) of IRSOFC operating on wet palm-BDF ($S/C = 3.5$) at 800°C was monitored during the durability test. In Table 9, the composition of the anode off-gas and open circuit voltage (OCV) just before the durability test are listed together with the equilibrium gas composition estimated by HSC 5.1 software (Outokumpu Research Oy, Finland) and the theoretical electromotive force calculated by Nernst equation. Internal steam reforming of palm-BDF led to H_2 rich reformate gas, indicating that syngas as well as electricity can be obtained directly from BDF using high temperature SOFC. Measured concentrations of H_2 , CO and CO_2 were close to the calculated values. The initial OCV, 0.93 V , was close to the thermodynamic value of 0.94 V . The existence of methane and ethylene indicates that the internal steam reforming has not reached equilibrium. Especially, ethylene is well known as a precursor of carbon deposition (Yoon et al., 2008, 2009).

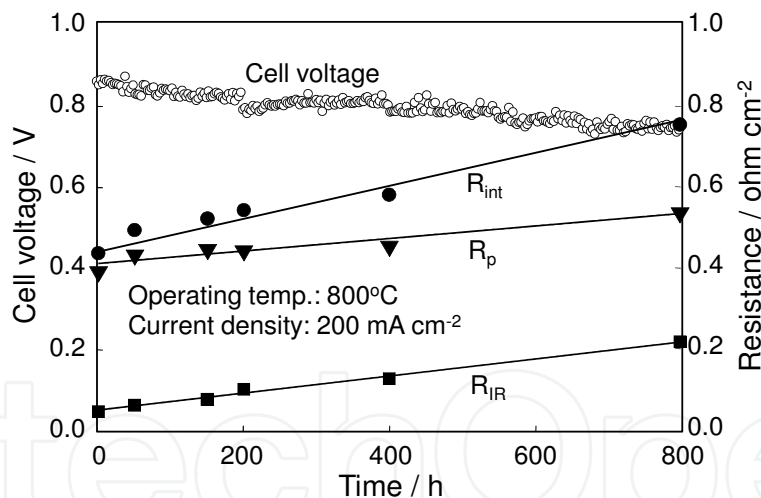


Fig. 12. The result of long term test of IRSOFC operating on wet palm-BDF ($S/C = 3.5$) at 800°C , showing cell voltage, total ohmic resistance R_{IR} , total polarization resistance R_P and internal resistance of the cell R_{int} during the test.

	Outlet gas concentration (dry basis) / %					OCV / V
	H_2	CO	CO_2	CH_4	C_2H_4	
Measured	65.3	14.9	15.0	2.3	2.5	0.93
Calculated	70.8	14.4	14.8	0	0	0.94

Table 9. Anode off-gas composition and OCV for an IRSOFC operating on palm-BDF operated at 800°C just before the durability test shown in Fig. 12.

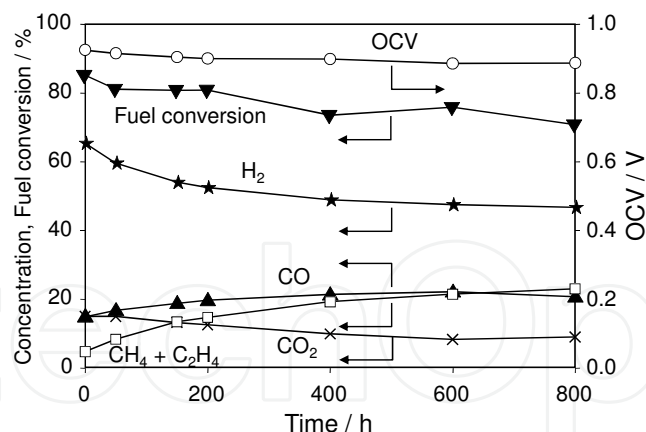


Fig. 13. Time dependence of OCV, fuel conversion and anode off-gas composition under open-circuit condition during the long term test of an IRSOFC operating on wet palm-BDF ($S/C = 3.5$) at 800°C shown in Fig. 12.

Figure 13 shows the concentrations of the gaseous species in the anode off-gas, fuel conversion and OCV during the long term test of Fig. 12. Although OCV was stable over the test, H_2 production rapidly degraded within the first 400 h. At least 800 h was necessary for the stabilization of the internal steam reforming of palm-BDF.

After stopping the supply of palm-BDF, cell temperature was decreased to room temperature under the thorough N_2 purging of the anode compartment. FESEM images of the (a) surface and (b) cross section of the anode support after the long term test are shown in Fig. 14. Carbon deposition occurred only on the surface of the anode which is most susceptible to coking due to the highest concentration of long chain hydrocarbons or lowest S/C , whereas inside of the porous anode support there was no coke. The occurrence of electrochemical consumption of H_2 leading to an increase in local S/C and direct electrochemical consumption of carbon may prevent coking inside of the anode. Carbon deposited on the anode surface can push up the current collector mesh attached to the anode surface resulting in the R_{IR} increase shown in Fig. 12.

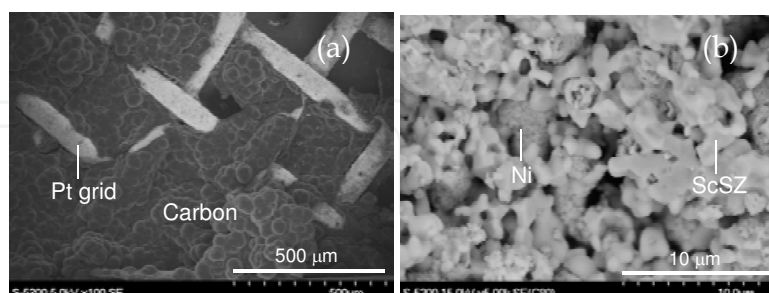


Fig. 14. FESEM images of (a) surface and (b) inside of the porous anode support after 800 h test of IRSOFC operating on wet palm-BDF ($S/C = 3.5$) at 0.2 A cm^{-2} and 800°C .

4.3 Problems to be solved for the realization of *Bio*-SOFCs

The feasibility of an IRSOFC running on low-grade biofuels has been demonstrated in the previous research (Shiratori et al., 2010a, 2010b, 2011) using anode-supported button cells. However, as illustrated in Fig. 15, in the real SOFC system a strong temperature gradient along gas flow direction exists and can cause cell fracture.

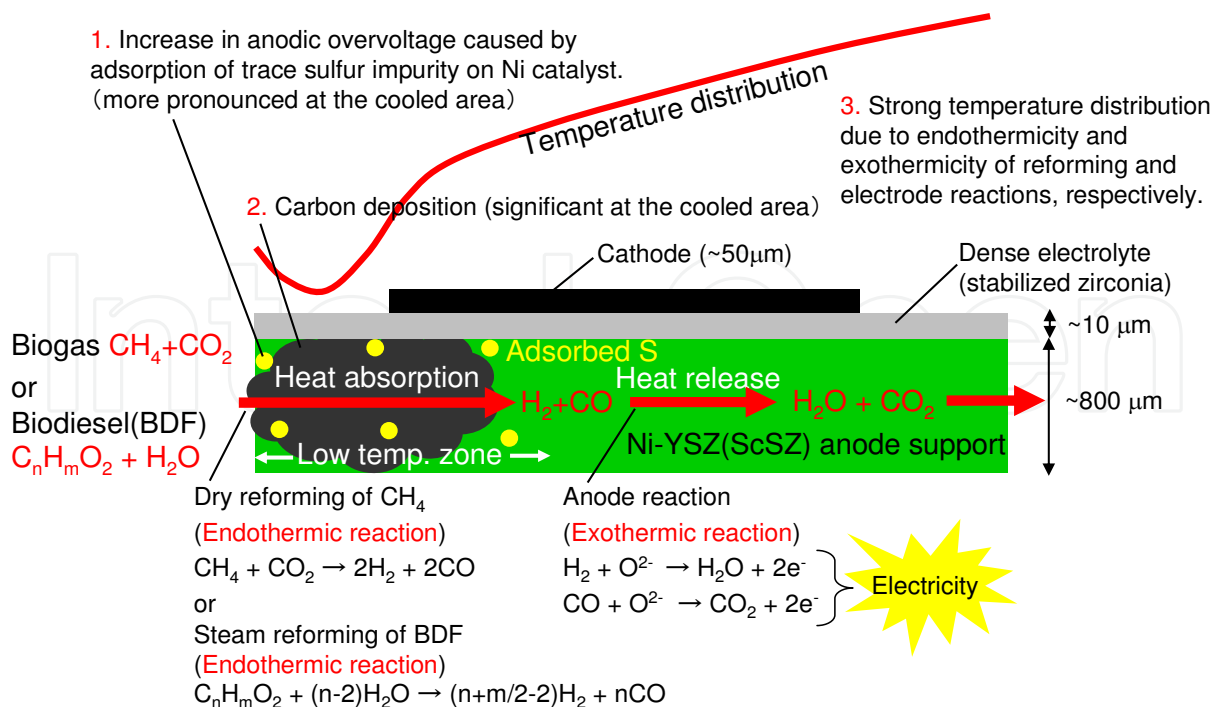


Fig. 15. Schematic view of *Bio*-SOFC and major problems to be solved.

The area near the fuel inlet is cooled down due to the strong endothermicity of reforming reactions (dry and steam reforming reactions of hydrocarbons), whereas cell temperature is gradually elevated toward the gas outlet by the exothermic electrochemical reactions. It is thermodynamically expected that impurity poisoning and carbon deposition are more significant at the cooled area.

4.3.1 Impurity poisoning (a case study of biogas operation)

Generally biofuels including biogas and BDFs contain several kinds of impurities such as sulfur compounds. According to thermochemical calculations (Haga et al., 2008), sulfur compounds exist as H_2S at SOFC operational temperatures in equilibrium. Here, in order to investigate the influence of a fuel impurity, 1 ppm H_2S was mixed with simulated biogas mixture ($\text{CH}_4/\text{CO}_2 = 1.5$) during the galvanostatic measurement under 200 mA cm^{-2} . CO yield and selectivity were measured simultaneously with the electrochemical measurements. CO yield and selectivity are defined as

$$\text{CO yield} = v_{\text{CO}} / (f_{\text{CH}_4} + f_{\text{CO}_2}) \quad (6)$$

$$\text{CO selectivity} = v_{\text{CO}} / (v_{\text{CH}_4} + v_{\text{CO}_2}) \quad (7)$$

where v_{CO} is CO formation rate, and f_{CH_4} and f_{CO_2} are feeding rates of CH_4 and CO_2 , respectively, and v_{CH_4} and v_{CO_2} are consumption rates of CH_4 and CO_2 , respectively. v_{CO} , v_{CH_4} and v_{CO_2} were estimated from the results of the exhaust gas analysis. The results of H_2S poisoning test at $1000 \text{ }^\circ\text{C}$ are summarized in Fig. 16.

In this experiment, an electrolyte-supported cell was used to measure anodic overvoltage separately from cathodic overvoltage using a Pt reference electrode (Shiratori, 2008). The horizontal axis indicates the time after starting poisoning. As shown in Fig. 16a even if 1 ppm H_2S was included in biogas, a cell voltage of about 1 V was stable during 20 h

operation while voltage drop of about 100 mV (9 % of initial cell voltage) occurred in the first 1 h. The voltage drop was caused by increase in anodic overvoltage. Just after starting 1 ppm H₂S poisoning, anodic overvoltage grew to be 3.6 times larger compared to the initial value, which would be due to sulfur surface coverage of Ni catalysts. On the other hand, the anode-side IR drop did not change by the H₂S poisoning.

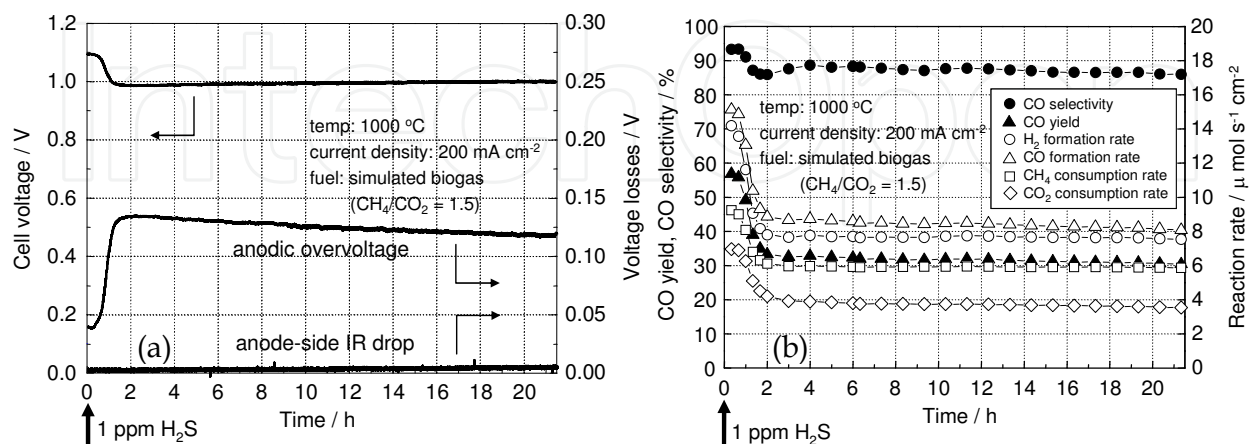


Fig. 16. Electrochemical and catalytic performance of Ni-ScSZ anode during 1 ppm H₂S poisoning measured at 1000 °C under 200 mA cm⁻²; (a) cell voltage, anodic overvoltage (IR free) and anode-side IR drop and (b) reaction rates, CO yield and CO selectivity for internal dry reforming of methane. Simulated biogas mixture, CH₄/CO₂ = 1.5, was fed as a fuel (Shiratori et al., 2008).

The reaction rates of internal reforming, CO yield and CO selectivity during 1 ppm H₂S poisoning test are plotted on Fig. 16b. Rapid deactivation of the reforming reaction was observed within 2 h after starting H₂S poisoning resulting in about a 40 % decrease in reaction rates and CO yield. On the other hand, CO selectivity was less sensitive to H₂S contamination (only 7 % decrease). After the initial deactivation of the catalytic activity, a quasi-stable state appeared. Fig. 17 schematically depicts the degradation mechanism of an IRSOFC operating on biogas under H₂S contamination. Sulfur species chemisorbed on Ni catalyst not only deactivate reforming reaction but also block the triple phase boundary (TPB) which is the active reaction region for electrochemical oxidation of produced H₂ and CO. Deactivation of reforming reaction causes deficiency of H₂ and CO, and blockage of TPB sites causes an increase in local current density. These phenomena would appear as an initial increase in anodic overvoltage (or initial voltage drop). Cell voltage, CO yield and CO selectivity completely recovered within 4h after stopping H₂S poisoning, indicating that H₂S poisoning caused by adsorption of sulfur species is a reversible process and 1 ppm level H₂S contamination is not fatal for the operation of Bio-SOFC at 1000 °C.

On the contrary, at 800 °C, 1 ppm H₂S was more detrimental. Cell voltage and internal reforming rates kept on decreasing during 22 h of H₂S poisoning. Voltage drop of about 170 mV (20 % of initial cell voltage) and 80 % decrease in the reaction rates occurred without the quasi-stable state as in the case of 1000 °C testing. The results summarized in Table 10 indicate that higher-grade desulfurization is required for lower operating temperatures, suggesting that the effect of impurity poisoning will become more detrimental at the cooled area in the cell (see Fig. 15).

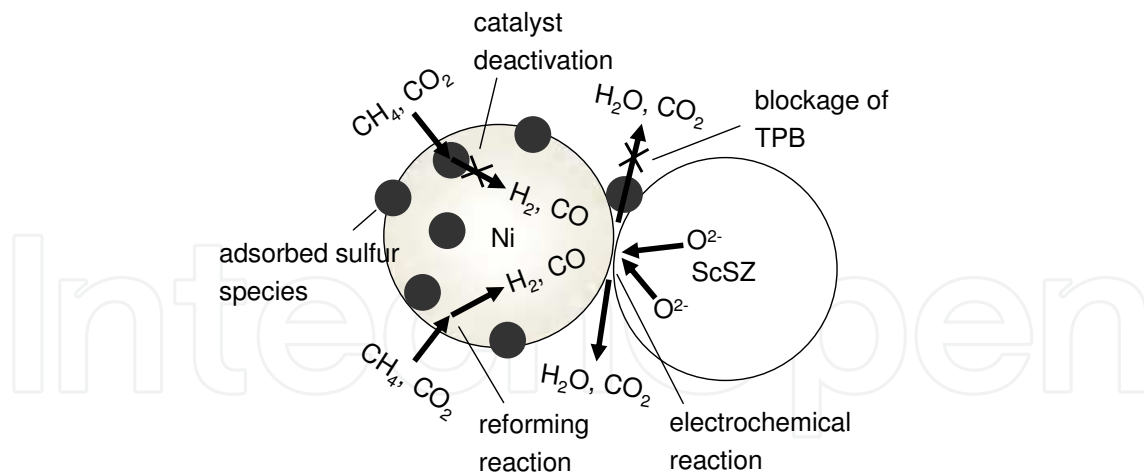


Fig. 17. Possible degradation mechanism of IRSOFC operating on biogas caused by H₂S contamination of biogas (Shiratori et al., 2008).

Temp.	Cell voltage	IR loss	Syngas production	Degradation behavior
1000 °C (Electrolyte-supported)	9 % decrease (100 mV)	not changed	40 % decrease	initial voltage drop followed by quasi-stable state
800 °C (Anode-supported)	20 % decrease (170 mV)	not changed	80 % decrease	continuous degradation

Table 10. Impact of 1 ppm H₂S contamination of biogas on the performance of IRSOFC running on biogas deduced by the 22 h poisoning test. Fuel: simulated biogas mixture (CH₄/CO₂ = 1.5), Cell: Ni-ScSZ/ScSZ/LSM-ScSZ (Shiratori et al., 2009a).

4.3.2 Strong temperature gradient (a case study of biogas operation)

Ni-ScSZ/ScSZ/LSM-ScSZ square-shaped cells with an area of 25 cm² simulating a real SOFC were used for the evaluation of thermomechanical reliability of a *Bio*-SOFC. When the simulated biogas (CH₄/CO₂ = 1.5) was directly fed to the square-shaped cell, long term operation could not be performed at 800 °C (Shiratori et al., 2010b). This is due to a locally-decreased cell temperature caused by the strong endothermicity of internal reforming (Fig. 15).

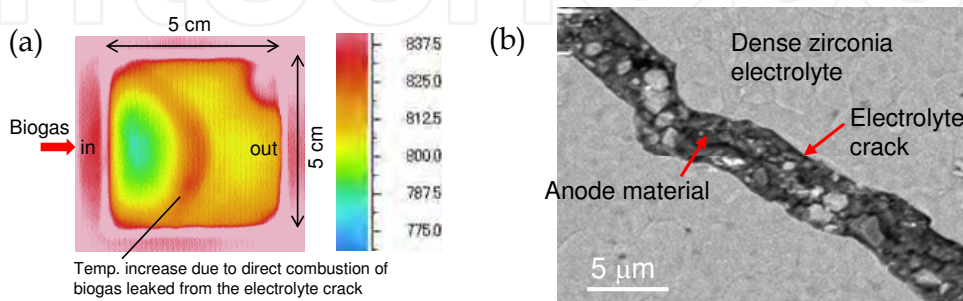


Fig. 18. (a) The temperature distribution caused by internal dry reforming of methane and (b) resulting cell fracture detected by FESEM, showing brittleness of electrolyte thin film sintered on the anode support versus direct supply of hydrocarbon fuel.

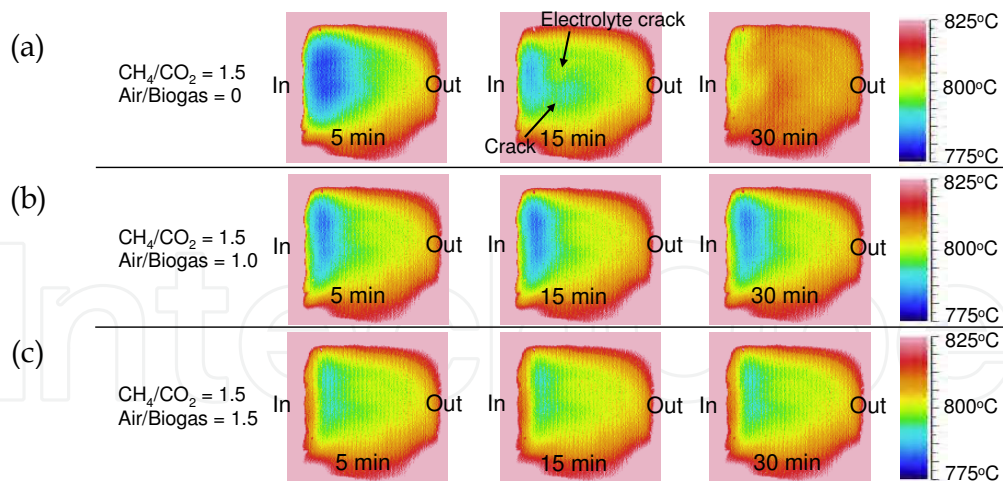


Fig. 19. The temperature distribution in the Ni-ScSZ anode support when simulated biogases with $\text{CH}_4/\text{CO}_2 = 1.5$ were fed directly with a furnace temperature of 800°C under open circuit condition; (a) Air/Biogas = 0, (b) 1.0 and (c) 1.5.

To estimate the endothermicity of reaction 1 in Table 7, an equimolar mixture of CH_4 and CO_2 was supplied to the square-shaped anode-supported half cell, and the temperature distribution generated in the half cell was measured from the electrolyte side by thermography. As shown in Fig. 18a, a large temperature gradient was generated at the fuel inlet side, and the temperature around the cooled area considerably increased within 20 min, indicating the formation of an electrolyte crack (Fig. 18b) from which biogas leaked and burned. When simulated biogas with $\text{CH}_4/\text{CO}_2 = 1.5$ was used as a fuel, at a furnace temperature of 800°C , as shown in Fig. 19a, a strong temperature gradient formed in the half cell and led to an electrolyte crack within 15 min after starting the supply of simulated biogas. The temperature gradient became more moderate with air addition to the biogas, as can be seen in Fig. 19b and c, for air/biogas of 1.0 and 1.5, respectively, at the same furnace temperature.

Reaction		Reaction enthalpy at 1100 K / kJ mol^{-1}
1	$\text{CH}_4 + \text{CO}_2 \rightarrow 2\text{H}_2 + 2\text{CO}$ Dry reforming of methane	259
2	$\text{CH}_4 + 1/2\text{O}_2 \rightarrow 2\text{H}_2 + \text{CO}$ Partial oxidation of methane	-23
3	$\text{CH}_4 + 2\text{O}_2 \rightarrow 2\text{H}_2\text{O} + \text{CO}_2$ Complete oxidation of methane	-802
4	$\text{CH}_4 + \text{H}_2\text{O} \rightarrow 3\text{H}_2 + \text{CO}$ Steam reforming of methane	226
5	$\text{CH}_4 \rightarrow \text{C} + 2\text{H}_2$ Methane cracking	90
6	$2\text{CO} \rightarrow \text{C} + \text{CO}_2$ Boudouard reaction	-170
7	$\text{CO} + \text{H}_2\text{O} \rightarrow \text{H}_2 + \text{CO}_2$ Water-gas-shift reaction	-34
8	$\text{CO} + 1/2\text{O}_2 \rightarrow \text{CO}_2$ Oxidation of carbon monoxide	-282
9	$\text{H}_2 + 1/2\text{O}_2 \rightarrow \text{H}_2\text{O}$ Oxidation of hydrogen	-248

Table 11. Main reactions involved in the reforming of air-mixed biogas and their reaction enthalpies at 1100 K (D.R. Lide (Ed.), 2009).

The above results indicate that cell performance can be stabilized by addition of air to biogas as a result of the exothermicity of partial oxidation of CH_4 . Here, heat absorption accompanied by the internal reforming of air-mixed biogas was calculated thermodynamically for the feed of 1 kmol C considering the reactions listed in Table 11. Reactions 1-3 are the predominant reactions determining the amount of heat absorption. Reaction 1 is dry reforming of CH_4 , producing H_2 and CO , which is a strong endothermic reaction. Reactions 2 and 3 are oxidation reactions of CH_4 which can contribute to the suppression of the strong endothermicity of reaction 1. The results of the thermodynamic calculation are plotted on Fig. 20.

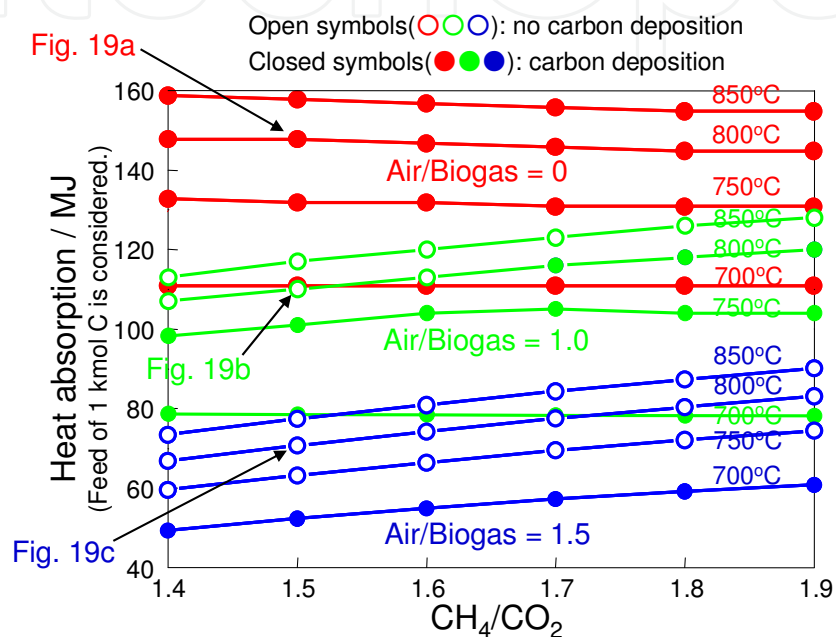


Fig. 20. Endothermicity of reforming of air-mixed biogases with Air/Biogas = 0, 1.0 and 1.5.

Fig. 20 suggests that heat absorption or endothermicity can be suppressed by increasing the air mixing ratio or by decreasing the operational temperature. A homogeneous temperature distribution obtained for Air/Biogas = 1.5 (Fig. 19c) as compared to Air/Biogas = 0 (Fig. 19a) is due to a 48 % lower heat absorption. Here, it is noted that the addition of excess air will result in the reduction of reforming efficiency, and lower operating temperature tends to cause carbon formation. The optimum Air/Biogas and operating temperature must be determined carefully, considering these points.

4.3.3 Carbon deposition

4.3.3.1 Biogas

The result of a long term test with a square-shaped cell is shown in Fig. 21a (Shiratori et al., 2010b). A degradation rate of 2.6 %/1000 h (200-500 h) was achieved by feeding air-mixed simulated biogas. The reasons for the degradation were a decrease in OCV (contribution ratio = 38 %) caused by incomplete gas sealing around the cell and increases in IR loss (34 %) and overvoltage (29 %) caused by insufficient electrical contact between the anode support and current collector. These voltage losses are related to technical difficulties of single cell testing with a square-shaped cell.

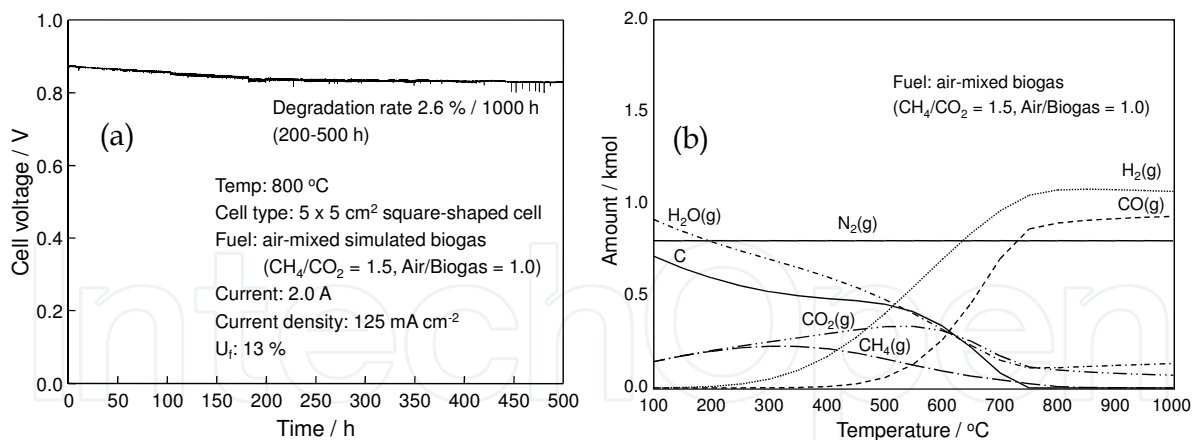


Fig. 21. Long-term test of an IRSOFC operating on biogas using a $5 \times 5 \text{ cm}^2$ square-shaped cell: (a) galvanostatic measurement of cell voltage in air-mixed simulated biogas ($\text{CH}_4/\text{CO}_2 = 1.5$, Air/Biogas = 1) under $U_f = 13\%$ at $800 \text{ }^\circ\text{C}$ and (b) the equilibrium gas composition calculated by HSC 5.1 software (Outokumpu Research Oy, Finland) for $0.6 \text{ kmol CH}_4 + 0.4 \text{ kmol CO}_2 + 0.2 \text{ kmol O}_2 + 0.8 \text{ kmol N}_2$.

As shown in Fig. 21b, at $800 \text{ }^\circ\text{C}$ (operational temperature in the present study) direct feeding of air-mixed biogas ($\text{CH}_4/\text{CO}_2 = 1.5$, Air/Biogas = 1) thermodynamically does not cause carbon deposition. The safe temperature region for this fuel is above $750 \text{ }^\circ\text{C}$, and a decrease in cell temperature over 50 K from the operational temperature of $800 \text{ }^\circ\text{C}$ may cause carbon deposition. After the 500 h durability test, carbon deposition was observed only at the fuel inlet side where the anode-support may be cooled down by more than 50 K as a result of the endothermic reforming reaction (Shiratori et al., 2010b). According to the thermodynamic calculation shown in Fig. 20, only 26% reduction of heat absorption is expected by the addition of an equimolar amount of air to biogas (Air/Biogas = 1.0). These results suggest that Air/Biogas = 1.0 is a thermodynamically safe composition if the temperature of $800 \text{ }^\circ\text{C}$ is kept anywhere in the anode-support, however taking the temperature gradient caused by the internal reforming into account, Air/Biogas = 1.0 leads to a decrease in the cell temperature at the fuel inlet side by more than 50 K , but is insufficient, Air/Biogas ratio higher than 1.0 is required practically.

4.3.3.2 Biodiesel fuels (BDFs)

Figure 22 shows the results of galvanostatic measurements at three different operating temperatures for palm-, jatropha- and soybean-BDFs under the condition of 200 mA cm^{-2} and $S/C = 3.5$. Stable voltage with little oscillation was obtained only for palm-BDF at $800 \text{ }^\circ\text{C}$. In contrast, jatropha- and soybean-BDFs resulted in unstable cell voltage. Especially, at $700 \text{ }^\circ\text{C}$, cell voltage for the SOFCs operating on jatropha- and soybean-BDFs dropped abruptly within 40 h and 47 h , respectively. No severe coking was observed at $800 \text{ }^\circ\text{C}$ in the case of palm-BDF, whereas jatropha- and soybean-BDFs led to significant amount of carbon on the anode surface. Carbon deposition tended to be more significant at lower operating temperatures and at higher content of unsaturated FAMES in BDF.

Figure 23 shows the anode surface after the operation with real biodiesels at $800 \text{ }^\circ\text{C}$. Nearly no carbon was observed at this temperature in the case of palm-BDF, whereas jatropha- and soybean-BDFs led to significant amount of carbon on the anode surface. Carbon deposition tended to be more significant for the fuels with a higher degree of unsaturation (Nahar,

2010). The rapid degradation is due to the carbon deposition promoted with a higher degree of unsaturation which can cover a portion of active reaction sites or block open pores.

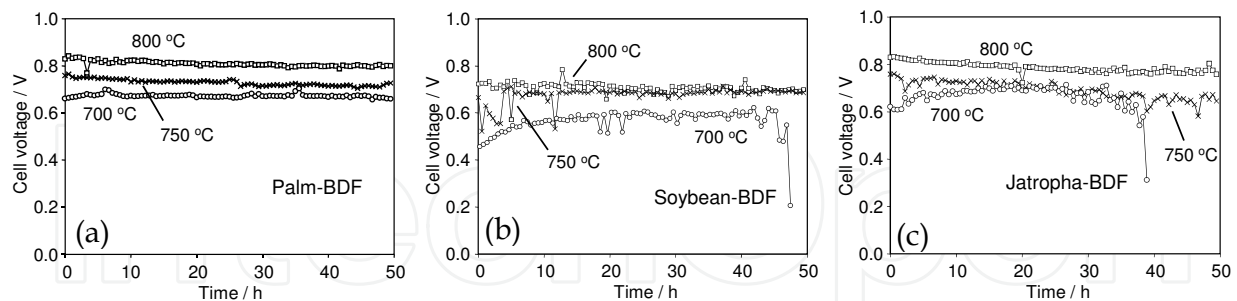


Fig. 22. Cell voltage of IRSOFCS operating on (a) palm-, (b) jatropha- and (c) soybean-BDFs at different temperatures under the condition of $S/C = 3.5$ and 200 mA cm^{-2} .

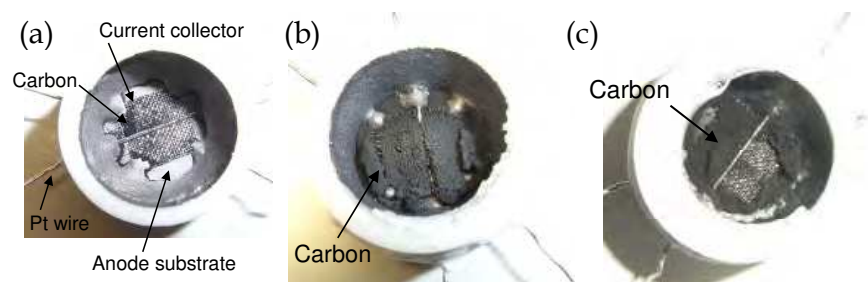


Fig. 23. Pictures of the anode after the 50 h tests of IRSOFCS operating on BDFs at $800 \text{ }^\circ\text{C}$ shown in Fig. 22; (a), (b) and (c) are for palm-, jatropha- and soybean-BDFs, respectively.

5. Conclusion

The fuel flexibility of SOFCs has been demonstrated in this study with biofuels, biogas and biodiesel fuels (BDFs). In the course of this study, roadblocks for the realization of an internal reforming SOFC (IRSOFCS) operating on biofuels, *Bio*-SOFC, which is promising candidate for a distributed generator in a coming carbon-neutral society, were uncovered. A biogas-fueled SOFC can be operated internal reforming mode if an adequate amount of air is added to the biogas. To suppress carbon deposition and thermal stress caused by the internal reforming reaction, $\text{Air/Biogas} > 1.0$ is required. Although the feasibility of an IRSOFCS running on biogas has been demonstrated in the previous research, there is an urgent need to collect more practical data using a real stack. On the other hand, performance of an IRSOFCS operating on BDFs has also been evaluated. The deactivation of the anode was accompanied by significant carbon deposition on the Ni-based anode material, which occurs more for lower operating temperature and higher concentration of unsaturated fatty acid methyl esters (FAMES) in BDF. Only the IRSOFCS operating on palm-BDF with the lowest degree of unsaturation operated at $800 \text{ }^\circ\text{C}$ exhibited stable performance without severe coking. The concentration of unsaturated FAMES in BDF is quite an important factor to determine SOFC performance, and therefore it should be controlled carefully. In terms of fuel injection performance, a higher concentration of unsaturated components resulting in lower viscosity of BDFs is preferable, however significant carbon deposition will occur as mentioned above.

Our final goal is to operate an IRSOFC using low grade biofuels. BDF derived from waste cooking oil which has a similar chemical composition to that of palm-BDF is quite an attractive candidate for SOFC operation, although the fuel composition fluctuates depending on the origin of the oil and kind of food cooked by the oil. On the other hand, south-east Asian nations near the Mekong basin are very interested in the efficient use of their abundant fishery resources as alternative fuels. BDF derived from discarded catfish oil is one of the most attractive alternative fuels, however it contains not only FAMES with high number of carbon atom between 20 and 24 in a molecule, but also several trace impurities which promote carbon deposition. In future work, the dependence of IRSOFC performance on composition of BDFs will be investigated.

6. Acknowledgement

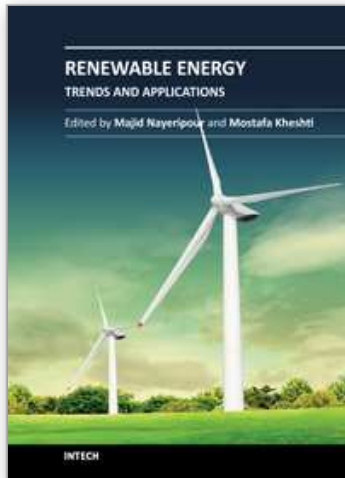
The authors are deeply grateful to Saga prefecture for their financial support to carry out this research and Tosu Kankyo Kaihatsu Inc. for their cooperation in operating the methane fermentation reactor.

7. References

- Byham, S.; Spendelow, J.; Martin, K. E.; Ho, D. L.; Marcinkoski, J. & Papageorgopoulos, D. (2010). U.S. Department of energy activities in supporting fuel cell technologies for CHP and APU applications. in *9th European SOFC Forum*, Connor, P.; Irvine, J.; Cassidy, M.; Savaniu, C.; Smith, M. & Knowles, S. Editors, pp.2.1-2.11, European Fuel Cell Forum Proceedings Series, Switzerland, 2010.
- Föger, K. (2010). Commercialisation of CFCL's residential power station BluGen. in *9th European SOFC Forum*, Connor, P.; Irvine, J.; Cassidy, M.; Savaniu, C.; Smith, M. & Knowles, S. Editors, pp.2.22-2.28, European Fuel Cell Forum Proceedings Series, Switzerland, 2010.
- Gardner, F.J.; Day, M.J.; Brandon, N.P.; Pashley, M.N. & Cassidy, M. (2000). SOFC technology development at Rolls-Royce. *Journal of Power Sources*, 86:122-129, ISSN 0378-7753.
- Girona, K.; Laurencin, J.; Petitjean, M.; Fouletier, J. & Lefebvre-Joud, F. (2009). SOFC running on biogas: identification and experimental validation of "Safe" operating conditions. *ECS Transactions*, 25(2):1041-1050, ISSN 1938-5862.
- Haberman, B. A.; Baca, C. M. & Ohrn, T. R. (2011). IP-SOFC performance measurement and prediction. *ECS Transactions*, 35(1):451-464, ISSN 1938-5862.
- Haga, K.; Adachi, S.; Shiratori, Y.; Itoh, K. & Sasaki, K. (2008). Poisoning of SOFC anodes by various fuel impurities. *Solid State Ionics*, 179:1427-1431, ISSN 0167-2738.
- Hosoi, K.; Ito, M. & Fukae, M. (2011). Status of national project for SOFC development in Japan. *ECS Transactions*, 35(1):11-18, ISSN 1938-5862.
- Huang, P. & Ghezal-Ayagh, H. (2011). SOFC module material development at fuel cell energy. *ECS Transactions*, 35(1):2631-2638, ISSN 1938-5862.
- Iida, T.; Kawano, M.; Matsui, T.; Kikuchi, R. & Eguchi, K. (2007). Internal reforming of SOFCs: carbon deposition on fuel electrode and subsequent deterioration of cell. *Journal of Electrochemical Society*, 154(2):B234-B241, ISSN 1945-7111.
- Ke, K.; Gunji, A.; Mori, H.; Tsuchida, S.; Takahashi, H.; Ukai, K.; Mizutani, Y.; Sumi, H.; Yokoyama, M. & Waki, K. (2007). Effect of oxide on carbon deposition behavior of CH₄ fuel on Ni/ScSZ cermet anode in high temperature SOFCs. *Solid State Ionics*, 177:541-547, ISSN 0167-2738.

- Kim, H.; Park, S.; Vohs, J.M. & Gorte R.J. (2001). Direct oxidation of liquid fuels in a solid oxide fuel cell. *Journal of Electrochemical Society*, 148(7):A693–A695, ISSN 1945-7111.
- Kishimoto, H.; Yamaji, K.; Horita, T.; Xiong, Y.; Sakai, N.; Brito, M. & Yokokawa, H. (2007). Feasibility of liquid hydrocarbon fuels for SOFC with Ni-ScSZ anode. *Journal of Power Sources*, 172:67–71, ISSN 0378-7753.
- Komatsu, Y.; Kimijima, S. & Szmyd, J.S. (2009). A performance analysis of a solid oxide fuel cell-micro gas turbine hybrid system using biogas. *ECS Transactions*, 25:1061-1070, ISSN 1938-5862.
- Lanzini, A. & Leone, P. (2010). Experimental investigation of direct internal reforming of biogas in solid oxide fuel cells. *International Journal of Hydrogen Energy*, 35:2463-2476, ISSN 0360-3199.
- Leah, R.; Bone, A.; Selcuk, A.; Corcoran, D.; Lankin, M.; Dehaney-Steven, Z.; Selby, M. & Whalen, P. (2011). Development of highly robust, volume-manufacturable metal-supported SOFCs for operation below 600°C. *ECS Transactions*, 35(1):351-367, ISSN 1938-5862.
- Leone, P.; Lanzini, A.; Santarelli, M.; Cali, M.; Sagnelli, F.; Boulanger, A.; Scaletta, A. & Zitella, P. (2010). Methane-free biogas for direct feeding of solid oxide fuel cells. *Journal of Power Sources*, 195:239-248, ISSN 0378-7753.
- Lide, D.R. (Ed.). (2008). *CRC Handbook of Chemistry and Physics*, Taylor & Francis Inc., ISBN 978-1-4200-6679-1, USA.
- Mai, A.; Iwanschitz, B.; Weissen, U.; Denzler, R.; Haberstock, D.; Nerlich, V. & Schuler, A. (2011). Status of Hexis' SOFC stack development and the Galileo 1000 N micro-CHP system. *ECS Transactions*, 35(1):87-95, ISSN 1938-5862.
- Nahar, N. (2010). Hydrogen Rich Gas Production by the autothermal reforming of biodiesel (FAME) for utilization in the solid-oxide fuel cells: A Thermodynamic Analysis. *International Journal of Hydrogen Energy*, 35:8891-8911, ISSN 0360-3199.
- Park, S.; Cracium, R.; Vohs, J.M. & Gorte, R.J. (1999). Direct oxidation of hydrocarbons in a solid oxide fuel cell: I. methane oxidation. *Journal of Electrochemical Society*, 146(10):3603–3605, ISSN 1945-7111.
- Payne, R.; Love, J. & Kah, M. (2011). CFCL's BlueGen product. *ECS Transactions*, 35(1):81-85, ISSN 1938-5862.
- Sasaki, K. & Teraoka, Y. (2003). Equilibria in fuel cell gases: I. equilibrium compositions and reforming conditions. *Journal of Electrochemical Society*, 150(7):A878–A884, ISSN 1945-7111.
- Sasaki, K.; Haga, K.; Yoshizumi, T.; Minematsu, D.; Yuki, E.; Liu, R.-R.; Uryu, C.; Oshima, T.; Taniguchi, S.; Shiratori, Y.; & Ito, K. (2011). Impurity poisoning of SOFCs. *ECS Transactions*, 35(1):2805-2814, ISSN 2151-2051.
- Shiratori, Y.; Oshima, T. & Sasaki, K. (2008). Feasibility of direct-biogas SOFC. *International Journal of Hydrogen Energy*, 33:6316–6321, ISSN 0360-3199.
- Shiratori, Y.; Ijichi, T.; Oshima, T. & Sasaki, K. (2009a). Generation of electricity from organic bio-wastes using Solid Oxide Fuel Cell. *ECS Transactions*, 25(2): 1051-1060, ISSN 1938-5862.
- Shiratori, Y.; Kazunari, S.; Tran, Q.T. & Huynh, Q. (2009b). Application of biofuels to solid oxide fuel cell. *Proc. of the 2009 International Forum on Strategic Technologies*, pp. 89-93, Ho Chi Minh, Viet Nam, October 21-23, 2009.
- Shiratori, Y.; Ijichi, T.; Oshima, T. & Sasaki, K. (2010a). Internal reforming SOFC running on biogas. *International Journal of Hydrogen Energy*, 35:7905–7912, ISSN 0360-3199.
- Shiratori, Y.; Ijichi, T.; Oshima, T. & Sasaki, K. (2010b). Performance of internal reforming SOFC running on biogas. in *9th European SOFC Forum*, Connor, P.; Irvine, J.;

- Cassidy, M.; Savaniu, C.; Smith, M. & Knowles, S. editors, pp.4-77-4-87, European Fuel Cell Forum Proceedings Series, Switzerland, 2010.
- Shiratori, Y.; Tran, Q.T.; Takahashi, Y. & Sasaki, K. (2011). Application of biofuels to solid oxide fuel cell. *ECS Transactions*, 35(1):2641-2651, ISSN 2151-2051.
- Staniforth, J. & Kendall, K. (1998). Biogas powering a small tubular solid oxide fuel cell. *Journal of Power Sources*, 71(1-2):275-277, ISSN 0378-7753.
- Staniforth, J. & Kendall, K. (2000). Cannock landfill gas powering a small tubular solid oxide fuel cell - a case study. *Journal of Power Sources*, 86:401-403, ISSN 0378-7753.
- Steele, BCH & Heinzl A. (2001). Materials for Fuel-cell Technologies. *Nature*, 414:345-352, ISSN 0028-0836.
- Stöver, D.; Buchkremer, H.P. & Huijsmans, J.P.P. (2003) MEA/cell preparation methods: Europe/USA, In: *Handbook of Fuel Cells-Fundamentals, Technology and Applications*, Vielstich, W.; Lamm, A. & Gasteiger, H. A. (Eds.), 1015-1031, John Wiley & Sons Ltd., ISBN 0-471-49926-9, England.
- Tran, Q.T.; Shiratori, Y. & Sasaki, K. (2011). Feasibility of palm-biodiesel fuel for internal reforming Solid Oxide Fuel Cells. *International Journal of Energy Research* (submitted), ISSN 1099-114X.
- Van herle, J.; Membrez, Y. & Bucheli, O. (2004a). Biogas as a fuel source for SOFC co-generators. *Journal of Power Sources*, 127:300-312, ISSN 0378-7753.
- Van herle, J.; Maréchal, F.; Leuenberger, S.; Membrez, Y.; Bucheli, O. & Favrat, D. (2004b). Process flow model of solid oxide fuel cell system supplied with sewage biogas. *Journal of Power Sources*, 131:127-141, ISSN 0378-7753.
- Xuan, J.; Leung, M.K.H.; Leung, D.Y.C. & Ni, M. (2009) A review of biomass-derived fuel processors for fuel cell systems. *Renewable and Sustainable Energy Reviews*, 13:1301-1313, ISSN 1364-0321.
- Yentekakis, I.V. (2006). Open- and closed-circuit study of an intermediate temperature SOFC directly fueled with simulated biogas mixtures. *Journal of Power Sources*, 160:422-425, ISSN 0378-7753.
- Yoon, S.; Kang, I. & Bae, J. (2008). Effects of ethylene on carbon formation in diesel autothermal reforming. *International Journal of Hydrogen Energy*, 33:4780-4788, ISSN 0360-3199.
- Yoon, S.; Kang, I. & Bae, J. (2009). Suppression of ethylene-induced carbon deposition in diesel autothermal reforming. *International Journal of Hydrogen Energy*, 34:1844-1851, ISSN 0360-3199.
- Yoshida, S.; Kabata, T.; Nishiura, M.; Koga, S.; Tomida, K.; Miyamoto, K.; Teramoto, Y.; Mataka, N.; Tsukuda, H.; Suemori, S.; Ando, Y. & Kobayashi, Y. (2011). Development of the SOFC-GT combined cycle system with tubular type cell stack. *ECS Transactions*, 35(1):105-111, ISSN 1938-5862.
- Yuki, E.; Haga, K.; Shiratori, Y.; Ito, K. & Sasaki K. (2009). Co-poisoning effects by sulfur impurities and hydrocarbons in SOFCs. *Proc. 18th Symposium on Solid Oxide Fuel Cells in Japan*, pp.104-107, Tokyo, Japan, December 2009.
- Zhou, Z.F.; Gallo, C.; Pargue, M.B.; Schobert, H. & Lvov S.N. (2004). Direct oxidation of Jet fuels and pennsylvania crude oil in a solid oxide fuel cell. *Journal of Power Sources*, 133:181-187, ISSN 0378-7753.
- Zhou, Z.F.; Kumar, R.; Thakur, S.T.; Rudnick, L.R.; Schobert, H. & Lvov, S.N. (2007). Direct oxidation of waste vegetable oil in solid-oxide fuel cells. *Journal of Power Sources*, 171:856-860, ISSN 0378-7753.
- Züttel, A. (2008). Material for the hydrogen world. in *Ceramic materials in energy system for sustainable development*, Gauckler, L.J. Editor. Forum 2008 of the World Academy of Ceramics, ISBN 978-88-86538-50-3, pp.211-260, Italy, 2008.



Renewable Energy - Trends and Applications

Edited by Dr. Majid Nayeripour

ISBN 978-953-307-939-4

Hard cover, 250 pages

Publisher InTech

Published online 09, November, 2011

Published in print edition November, 2011

Increase in electricity demand and environmental issues resulted in fast development of energy production from renewable resources. In the long term, application of RES can guarantee the ecologically sustainable energy supply. This book indicates recent trends and developments of renewable energy resources that organized in 11 chapters. It can be a source of information and basis for discussion for readers with different backgrounds.

How to reference

In order to correctly reference this scholarly work, feel free to copy and paste the following:

Yusuke Shiratori, Tran Tuyen Quang, Yutaro Takahashi, Shunsuke Taniguchi and Kazunari Sasaki (2011). Highly Efficient Biomass Utilization with Solid Oxide Fuel Cell Technology, Renewable Energy - Trends and Applications, Dr. Majid Nayeripour (Ed.), ISBN: 978-953-307-939-4, InTech, Available from: <http://www.intechopen.com/books/renewable-energy-trends-and-applications/highly-efficient-biomass-utilization-with-solid-oxide-fuel-cell-technology>

INTECH
open science | open minds

InTech Europe

University Campus STeP Ri
Slavka Krautzeka 83/A
51000 Rijeka, Croatia
Phone: +385 (51) 770 447
Fax: +385 (51) 686 166
www.intechopen.com

InTech China

Unit 405, Office Block, Hotel Equatorial Shanghai
No.65, Yan An Road (West), Shanghai, 200040, China
中国上海市延安西路65号上海国际贵都大饭店办公楼405单元
Phone: +86-21-62489820
Fax: +86-21-62489821

© 2011 The Author(s). Licensee IntechOpen. This is an open access article distributed under the terms of the [Creative Commons Attribution 3.0 License](#), which permits unrestricted use, distribution, and reproduction in any medium, provided the original work is properly cited.

IntechOpen

IntechOpen